*35th EPS Conference on Plasma Phys. Hersonissos, 9 - 13 June 2008 ECA Vol.**32D**, P-2.053 (2008)*

Numerical Analysis of Non-Resonant Pressure Driven Mode in Heliotron Plasma

K. Ichiguchi[1], B.A. Carreras[2]

[1] *National Institute for Fusion Science, Oroshi-cho 322-6, Toki 509-5292, Japan*

[2] *BACV Solutions Inc., 110 Mohawk, Oak Ridge, Tennessee 37831, USA*

Abstract : Linear and nonlinear properties of a non-resonant pressure driven mode localized around the magnetic axis in a heliotron plasma are studied numerically. The non-resonant mode is destabilized when there exist fairly large region around the magnetic axis with steep pressure gradient, rotational transform is close to the mode rational number and the magnetic shear is weak. The nonlinear analysis indicates that the mode can induce sawtooth-like oscillations.

1. Introduction

In the Large Helical Device (LHD) configuration with the vacuum magnetic axis located at 3.6m (R_{ax}=3.6m), sawtooth-like oscillations were observed with the soft X-ray camera system in fairly high density plasmas produced by pellet injection, although the effect of the MHD activity on the global confinement was small[1]. The instability is localized around the magnetic axis and has an $m = 3$ mode structure. For this magnetic configuration and as shown in Fig.1, there is no magnetic surface with $\iota = 1/3$. Therefore, there is a possibility that the mode observed experimentally is a non-resonant mode.

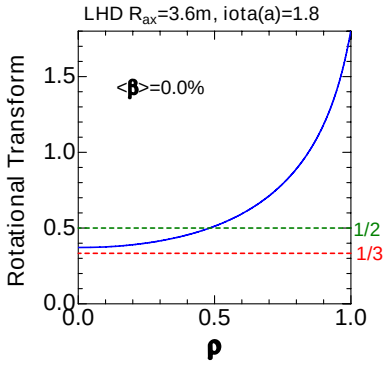

Figure 1: Rotational transform in vacuum LHD configuration with R_{ax}=3.6m.

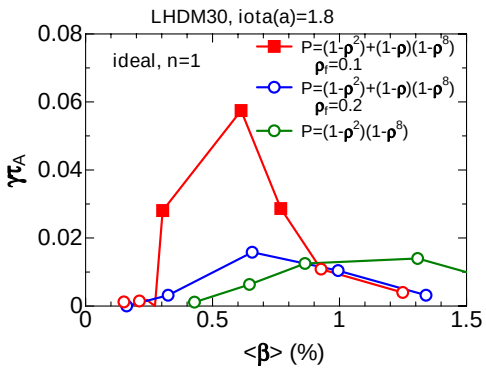

Figure 2: Growth rates of $n = 1$ ideal modes. Squares and circles denote (3,1) and (2,1) modes, respectively.

Here, we numerically study the properties of such a non-resonant mode. In this study, we analyze its linear ideal stability properties and its nonlinear dynamics in the beta increasing phase. We utilize the VMEC code[2] to calculate the three-dimensional equilibrium under the constraints of the free boundary and the no net-current. We utilize the NORM code[3, 4] for the linear stability and nonlinear dynamics of the mode. This code is based on the reduced MHD

equations.

2. Linear Stability Analysis

The unstable ideal non-resonant mode is obtained only for a steep pressure profile. Figure 2 shows the growth rate of the $n = 1$ ideal modes for the pressure profile given by

$$P(\rho) = P_0 \begin{cases} (1 - a\rho^2) & for \quad 0 \le \rho \le \rho_f \\ b(1-\rho)(1-\rho^8) & for \quad \rho_f \le \rho \le 1 \end{cases} \tag{1}$$

with $\rho_f = 0.1$. Here, ρ denotes a square-root of the normalized toroidal flux. The factors of a and b are determined so that the value and the first derivative of P are continuous at $\rho = \rho_f$. The growth rate for the profiles of eq.(1) with $\rho_f = 0.2$ and $P = P_0(1-\rho)(1-\rho^8)$ is also plotted as reference. A non-resonant $(m,n) = (3,1)$ mode is unstable only in the range of $0.3\% \lesssim \langle\beta\rangle \lesssim 0.8\%$ for the pressure profile of eq.(1) with $\rho_f = 0.1$. In other cases, the $(m,n) = (2,1)$ mode can be unstable. The non-resonant mode is also stable for the $P = P_0(1-\rho^2)^2$ and $P = P_0(1-\rho^2)^3$ profiles. The comparison of these pressure profile shown in Fig.3 indicates that a large pressure gradient around the magnetic axis is necessary for the destabilization of the mode. Hereafter, we focus on the pressure profile of eq.(1) with $\rho_f = 0.1$.

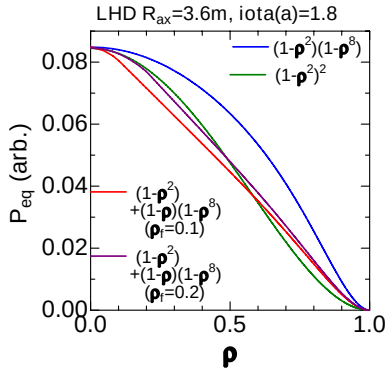

Figure 3: Pressure profiles examined in linear stability analysis.

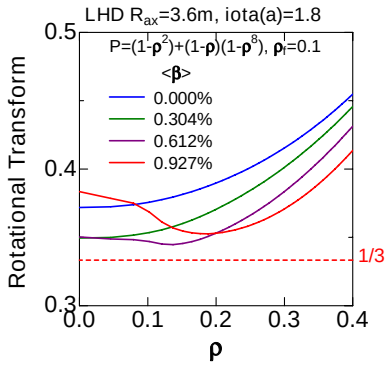

Figure 4: Beta dependence of rotational transform around the axis.

In order to investigate the equilibrium properties when the non-resonant mode is destabilized, we examine the beta dependence of the rotational transform. As shown in Fig.4, the rotational transform at the axis decreases and approaches to 1/3 for $\langle\beta\rangle \le 0.6\%$, and then increases as the beta value increases. Simultaneously, the magnetic shear is reduced in the region of $\rho \lesssim 0.2$ for $0.3\% \lesssim \langle\beta\rangle \lesssim 0.6\%$. Consequently, the non-resonant mode can be destabilized when the pressure profile is steep, the rotational transform is close to the rational number of the mode and the magnetic shear is weak around the axis. These features are similar to those of the infernal mode[5].

The non-resonant mode structure is quite different from that of the interchange mode. Figure 5 shows the profile of the stream function of the $n = 1$ mode for $\langle\beta\rangle = 0.612\%$. All components are localized around the magnetic axis. The sidebands of the mode are fairly large and the mode structure is similar to that of the ballooning mode. However, the contour of the perturbed pressure shows a clear $m = 3$ structure, as shown in Fig.6. This structure is consistent with the soft X-ray image shown in Ref.[1].

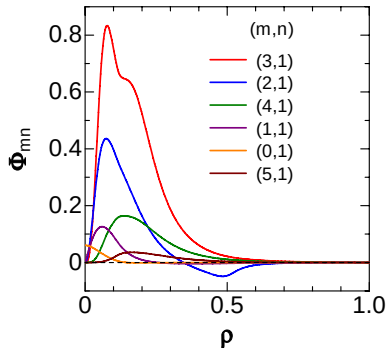

Figure 5: Stream function of $n = 1$ ideal mode at $\langle\beta\rangle = 0.612\%$.

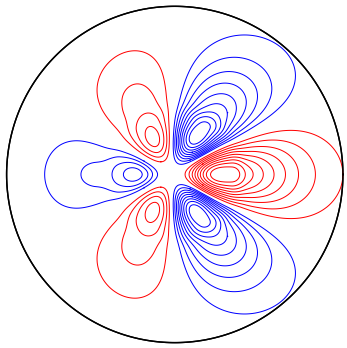

Figure 6: Contour of perturbed pressure at $\langle\beta\rangle = 0.612\%$ plotted in the region of $\rho \leq 0.3$.

3. Analysis of Non-Linear Dynamics with Multi-Scale Approach

In order to investigate whether the $(m,n) = (3,1)$ non-resonant mode is actually destabilized as a dominant mode, we examine the nonlinear behavior as beta increases. For this purpose, we utilize the multi-scale numerical scheme[6, 7]. In this scheme, both the effects of the nonlinear dynamics of the perturbation and the pressure increase due to an external source are incorporated in the time evolution of the pressure. In the present analysis, we assume the profile given by eq.(1) for the external pressure increment. We also assume the resistivity is such that $S = 10^6$.

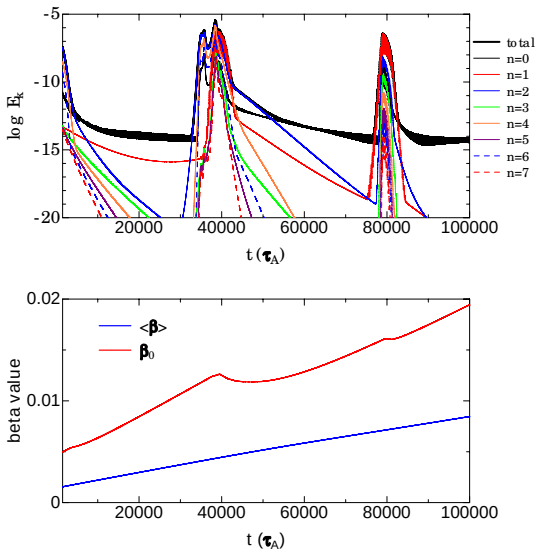

Figure 7: Time evolution of kinetic energy (top) and beta values (bottom).

Figure 7 shows the time evolution of the kinetic energy of the perturbation and the beta values for the LHD plasma with R_{ax}=3.6m. Two peaks appear during the time evolution of the kinetic energy at $t \sim 39000\tau_A$ and $t \sim 79000\tau_A$. The axis beta degrades after the kinetic energy peaks, while the average beta increases monotonously. The feature of the axis beta seems to be consistent with the experimental results[1] because the

axis beta shows a sawtooth-like behavior.

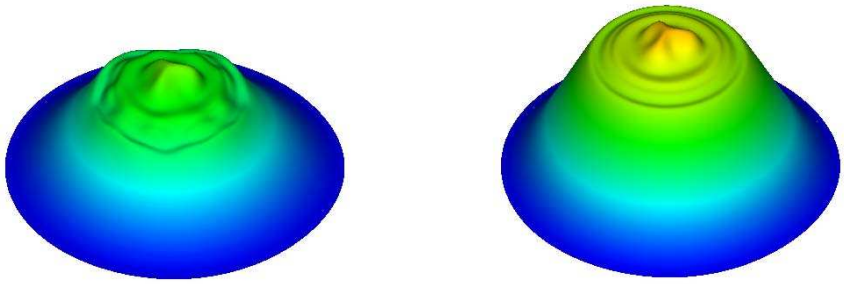

Figure 8: Bird's eye view of the pressure at $t = 39500\tau_A$ (left) and $t = 79500\tau_A$ (right).

The dominant mode is an $(m,n) = (3,1)$ mode at both peaks. The minimal value of the rotational transform is $\iota = 0.34613$ at $\rho = 0.03125$ for $t = 39950\tau_A$ ($\langle\beta\rangle = 0.442\%$) and $\iota = 0.34865$ at $\rho = 0.13020$ for $t = 79950\tau_A$ ($\langle\beta\rangle = 0.712\%$). In both cases, the magnetic shear is very weak in the region of $\rho \lesssim 0.2$. Hence, it is the $(m,n) = (3,1)$ non-resonant mode excited around the axis that causes the reduction of the axis beta. The total pressure profile around the axis is deformed into triangular shape, as shown in Fig.8.

4. Conclusions

The linear stability of the ideal non-resonant mode with $(m,n) = (3,1)$ is analyzed for the LHD configurations with R_{ax}=3.6m by using the NORM code. The mode becomes unstable only when the pressure profile is steep at a weak shear region with the rotational transform close to the rational value of the mode. This feature is similar to the infernal mode. The nonlinear dynamics of the non-resonant mode is also analyzed by applying the multi-scale approach. A degradation of confinement due to the mode is obtained. The time evolution of the beta value indicates a sawtooth-like activity, which seems to be consistent with the LHD experimental results.

Acknowledgments

This work is supported by NIFS cooperation programs NIFS07KLDD012 and by the Grant-in-Aid for Scientific Research (C) 17560736 of the Japan Society for the Promotion of Science.

References

[1] S. Ohdachi et al., Proc. Fusion Energy Conf. 2006, EX/P8-15.
[2] S.P. Hirshman, et al., Comput. Phys. Commun. **43**, 143-155 (1986).
[3] K. Ichiguchi, et al., Nucl. Fusion **43**, 1101-1109 (2003).
[4] K. Ichiguchi, et al., Fusion Science and Technology **46**, 34-43 (2004).
[5] *for example,* J. Manickam, et al., Nucl. Fusion **27**, 1461-1472 (1987).
[6] K. Ichiguchi, B. A. Carreras, J. Plasma Phys. **72** (2006) 1117-1121.
[7] K. Ichiguchi, B. A. Carreras, Plasma and Fusion Research **3** (2008) (in print).